Analyzing Benzene and Cyclohexane Emulsion Droplet Collisions on Ultramicroelectrodes

4 AUTHORS, INCLUDING:

Haiqiang Deng
École Polytechnique Fédérale de Lausanne

18 PUBLICATIONS   **83** CITATIONS

SEE PROFILE

Jeffrey E Dick
University of Texas at Austin

**14** PUBLICATIONS   **36** CITATIONS

SEE PROFILE

Analyzing Benzene and Cyclohexane Emulsion Droplet Collisions on Ultramicroelectrodes

Yan Li, Haiqiang Deng, Jeffrey E. Dick, and Allen J. Bard*

Center for Electrochemistry, Department of Chemistry, The University of Texas at Austin, 1 University Station A5300, Austin, Texas 78712, United States

S *Supporting Information*

ABSTRACT: We report the collisions of single emulsion oil droplets with extremely low dielectric constants (e.g., benzene, ε of 2.27, or cyclohexane, ε of 2.02) as studied via emulsion droplet reactor (EDR) on an ultramicroelectrode (UME). By applying appropriate potentials to the UME, we observed the electrochemical effects of single-collision signals from the bulk electrolysis of single emulsion droplets. Different hydrophobic redox species (ferrocene, decamethyl-ferrocene, or metalloporphyrin) were trapped in a mixed benzene (or cyclohexane) oil-in-water emulsion using an ionic liquid as the supporting electrolyte and emulsifier. The emulsions were prepared using ultrasonic processing. Spike-like responses were observed in each $i-t$ response due to the complete electrolysis of all of the above-mentioned redox species within the droplet. On the basis of these single-particle collision results, the collision frequency, size distribution, $i-t$ decay behavior of the emulsion droplets, and possible mechanisms are analyzed and discussed. This work demonstrated that bulk electrolysis can be achieved in a few seconds in these attoliter reactors, suggesting many applications, such as analysis and electrosynthesis in low dielectric constant solvents, which have a much broader potential window.
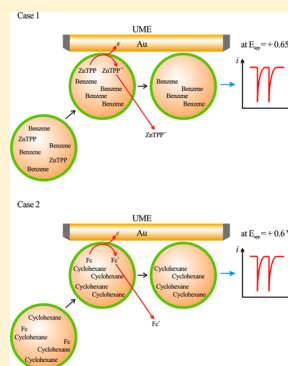
Microparticles and nanoparticles (NPs) have played a key role in many technical applications, such as catalysis, energy conversion and storage, spectroscopy, and the pharmaceutical industry.[1] These particles are conventionally characterized as an ensemble; thus, the performance of individual particles is poorly understood, and single particle peculiarities are averaged out during an ensemble analysis. In recent years, the electrochemistry of single-particle collisions has attracted increasing attention because of the important information, including the catalytic activity, size, and lifetime, which is not observable in ensemble samples but can be obtained at the single-particle level. Moreover, electrochemistry has been shown to be an efficient, cost-effective approach to collect such important information. The electrochemical study of single-collision events has been applied to a wide range of hard nanoparticles (NPs), including metals (Pt, Ag, Au, Cu, Ni),[2−7] metal oxides (IrO$_2$, TiO$_2$, CeO$_2$, SiO$_2$),[8−11] and organic NPs (indigo, polystyrene, and relatively large aggregates of fullerene).[12−14] Collisions of soft particles have also been investigated, such as toluene[15] and nitrobenzene droplets,[16] liposomes,[17] viruses,[18] vesicles,[19] and single macromolecules.[20]

Understanding single emulsion droplet collisions may also be of interest to many industrial applications (food processing, petroleum, and detergent industries).[21] The droplet size distribution of emulsion droplets influences many observed characteristics, such as the stability of the emulsion, rheology, optical properties, and sensory attributes, and is frequently measured.[22] Some methods for estimating the size distribution of emulsions have been established, including laser light scattering and microscopic methods.[23−25] However, laser light scattering methods usually cannot measure polydisperse

samples very well, and the overall result is an ensemble average over thousands of droplets. The microscopic method often requires dilution pretreatment, which is tedious and labor-intensive. Furthermore, wall effects (emulsion drop is flattened between two glass slides) need to be considered while employing a microscopic method.[21] Thus, the development of a method that provides information on single droplet chemistry is useful. In a previous publication, we reported the oxidation of ferrocene in toluene droplets dispersed in water on a gold ultramicroelectrode (UME).[15] Briefly, we employed oil emulsion droplets (e.g., toluene) containing hydrophobic redox molecules (e.g., ferrocene) and an ionic liquid that could collide with an UME in an aqueous continuous phase under an oxidation potential. Once the emulsion droplets collide, redox molecules inside the oil emulsion droplets start to be electrolyzed; thus, a spike-type current profile is observed in the current−time ($i-t$) measurements. In that study, we suggested the concept of the emulsion oil droplet as an attoliter electrochemical reactor for the electrochemistry of hydrophobic molecules in an aqueous continuous phase. Thus, the emulsion droplet reactor (EDR) serves as an attoliter electrolysis cell. We further explored the reduction electrochemistry inside a single emulsion droplet containing 7,7,8,8-tetracyanoquinodimethane (TCNQ), an ionic liquid, and nitrobenzene.[16] From these single emulsion collision results, we can obtain the collision frequency, size distribution, and $i-t$ decay behavior of the

emulsion droplets. These results will contribute to a better understanding of the collision of other types of single "soft" particles (liposomes and vesicles) on an UME, as demonstrated in previous papers.[17,19]

In this work, we report the electrochemical collisions of single emulsion oil droplets with extremely low dielectric constants (e.g., benzene and cyclohexane) based on EDR studies. The EDR method is very useful for studying low-volume reactors (attoliter),[26,27] collectors, and sensors; therefore, a deeper understanding of this EDR method is a prerequisite for its extensive applications. Here, various redox species (ferrocene, decamethyl-ferrocene, or metalloporphyrins) were trapped in a mixed benzene (or cyclohexane) oil-in-water emulsion using an ionic liquid as both the supporting electrolyte and the emulsifier. In this experiment, a spike in the current transient from the oxidation of the redox species was observed at the moment while an emulsion droplet collided with an UME (Figure 1). The key feature is that bulk
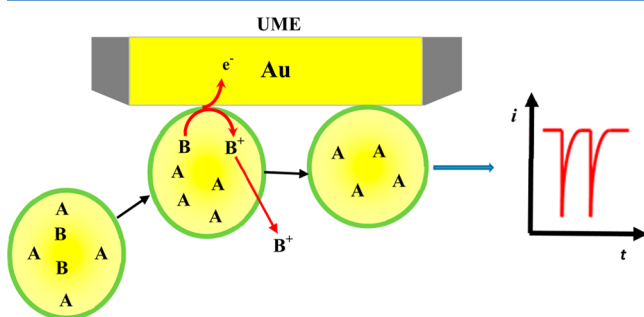

Figure 1. Schematic representation of the collisions of emulsion droplets containing solvent species A (benzene or cyclohexane) and hydrophobic electroactive species B (ferrocene, decamethyl-ferrocene, or metalloporphyrins). The yellow color corresponds to the oil phase. The green line suggests that some ionic liquid may form a layer at the oil/water interface. After oxidation of B, B$^+$ (or B$^{•+}$) leaves the droplet to maintain charge balance. The $i-t$ curve represented in the figure shows the electrochemical oxidation of hydrophobic electroactive species B in the droplet occurred at a 10 μm radius Au UME surface.

electrolysis can be achieved in a few seconds in these attoliter reactors, suggesting many applications, such as analysis and electrosynthesis in low dielectric constant solvents that exhibit a much broader potential window. These novel concepts and the experimental studies reported here increase our understanding of single droplet electrochemistry and stimulate new practical applications.

■ EXPERIMENTAL SECTION

Reagents and Materials. Benzene (99.8%), 5,10,15,20-tetraphenyl-21H,23H-porphine zinc (ZnTPP), ferrocene (98%), decamethyl ferrocene (DMFc) (97%), 5,10,15,20-tetraphenyl-21H,23H-porphine copper(II) (CuTPP), trihexyl-tetradecylphosphonium bis(trifluoromethylsulfonyl)amide (IL-PA) (≥95.0%), toluene (99.9%), and ethanol (99.9%) were obtained from Sigma-Aldrich (Figure 2). Cyclohexane (99.9%), concentrated sulfuric acid (95−98%), and hydrogen peroxide (30%) were obtained from Fisher Scientific. Au (99.99%) wire (10 μm diameter) was obtained from Goodfellow (Devon, PA). Millipore water (>18 MΩ·cm) was used throughout the experiments.

Instrumentation. The electrochemical experiments were performed using a CHI model 900B potentiostat (CH

Instruments, Austin, Texas) with a three-electrode cell placed in a Faraday cage. A 0.5 mm-diameter Pt wire was used as the counter electrode, with a silver wire as the quasireference electrode. A Q500 ultrasonic processor (Qsonica, Newtown, CT) with a microtip probe was used to create the emulsions. The dynamic laser scattering (DLS) studies were performed using a Zetasizer Nano ZS (Malvern, Westborough, MA).

Preparation of the UME. The Au UME was prepared following the general procedure developed in our lab. Briefly, a 10 μm Au wire was sealed in a borosilicate glass capillary after rinsing with ethanol and water. Then, the electrode was polished with an alumina (0.05 μm) powder−water suspension on a microcloth pad (Buehler, Lake Bluff, IL) to a mirror finish. The surface area was verified using the standard redox electrochemistry of ferrocenemethanol.

Preparation of the Benzene and Cyclohexane Emulsions. The benzene emulsions were prepared by dissolving ZnTPP (5 mM) and IL-PA (400 mM) in benzene (Figure S1A). The 0.15 mL mixture of benzene was added to 5 mL of distilled water. Then, the solution was vortexed vigorously for 20 s, and ultrasonic power (500 W, amplitude 40%) was immediately applied using the pulse mode (7 s on and 3 s off for 4 repeated cycles). The average diameter of the benzene (ZnTPP + IL-PA)/water emulsion droplets was 692 nm, as measured by DLS. The concentration of the benzene (ZnTPP + IL-PA)/water emulsion droplets was approximated by dividing the total benzene (ZnTPP + IL-PA) volume (0.15 mL) by the average emulsion droplet volume (173 aL, assumed to be spherical with a diameter of 692 nm). The benzene (ferrocene + IL-PA)/water emulsion droplets, benzene (decamethyl-ferrocene + IL-PA)/water emulsion droplets, and benzene (CuTPP + IL-PA)/water emulsion droplets were prepared as above, except a different redox species was used.

The cyclohexane emulsions were prepared by dissolving Fc (20 mM) and IL-PA (400 mM) in cyclohexane (Figure S1B). The 0.15 mL mixture of cyclohexane was added to 5 mL of distilled water. The ultrasonication procedure was the same as for the benzene emulsion system. The average diameter of the cyclohexane (Fc + IL-PA)/water emulsion droplets was 864 nm, as measured by DLS. The concentration of the cyclohexane (Fc + IL-PA)/water emulsion droplets was approximated from the total cyclohexane (Fc + IL-PA) volume (0.15 mL) divided by the average emulsion droplet volume (337.5 aL, assumed to be spherical with a diameter of 864 nm).

■ RESULTS AND DISCUSSION

Single Collision Events of Benzene Emulsion Droplets. *Electrochemical Oxidation of ZnTPP in Bulk Benzene Solution with 400 mM IL-PA as Supporting Electrolyte.* We used a benzene/water emulsion, which has been the subject of many studies. Benzene has a dielectric constant, ε, of 2.27, and supporting electrolytes for electrochemical studies in such a low dielectric medium are scarce; ion pairing of any electrolyte tends to produce very resistive solutions.[28] To solve this problem, the hydrophobic ionic liquid, IL-PA, has been used previously as the supporting electrolyte.[15] To compare the same reaction within an emulsion droplet, we used cyclic voltammetry (CV) to observe the oxidation of 5 mM ZnTPP in benzene with 400 mM IL-PA on a 10 μm Au UME (Figure S2). The CV shows a sigmoidal wave for the one-electron electrochemical oxidation of ZnTPP, and it is only slightly affected by the uncompensated resistance ($E_{3/4} - E_{1/4} = 72$
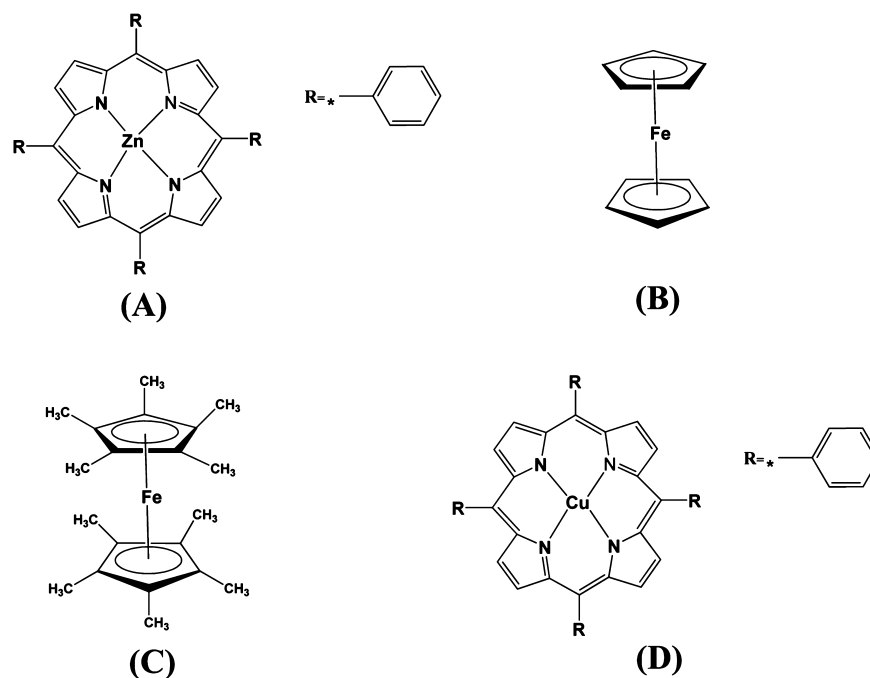
Figure 2. Molecular structure of (A) 5,10,15,20-tetraphenyl-21H,23H-porphine zinc (ZnTPP), (B) ferrocene (Fc), (C) decamethyl ferrocene (DMFc), and (D) 5,10,15,20-tetraphenyl-21H,23H-porphine copper(II) (CuTPP).

mV). The oxidation of ZnTPP begins at approximately +0.4 V (vs. Ag wire) and exhibits a steady-state current at approximately +0.65 V. The same benzene composition in 0.15 mL was mixed with 5 mL of water and was used to create the emulsion for the collision experiments. The as-prepared emulsion was stable for at least 24 h.

Collision Experiments of the Benzene (ZnTPP + IL-PA)/ Water Emulsion Droplets. Using chrono-amperometry, the collisions of benzene (ZnTPP + IL-PA)/water emulsion droplets on an Au UME were observed, resulting in the oxidation of ZnTPP to ZnTPP$^{\bullet+}$ inside the benzene emulsion droplets (Figure 3). As shown in Figure 3, a spike in the current response was clearly observed, which was ascribed to the electrolysis of ZnTPP in a single benzene emulsion droplet. Control experiments without ZnTPP in the droplet at an oxidation potential of 0.65 V produced no peaks (Figure S3). This observation supports the mechanism presented in Figure 1, which shows that current spikes are only observed when the electroactive species is oxidized. The collision frequency (f_{ems}) governed by the diffusion of the emulsion droplet can be calculated by eq 1,[15,29]

$$f_{ems} = 4D_{ems}C_{ems}r_{elec}N_A \tag{1}$$

where D_{ems} and C_{ems} are the diffusion coefficient and concentration of the droplets, r_{elec} is the radius of the working electrode, and N_A is Avogadro's number. The diffusion coefficient of the emulsion droplets (D_{ems}) can be estimated by the Stokes−Einstein equation (eq 2),

$$D_{ems} = \frac{k_B T}{6\pi\eta r_{ems}} \tag{2}$$

where k_B is the Boltzmann constant, T is temperature, η is the dynamic viscosity of water at 25 °C, and r_{ems} is the radius of an emulsion droplet. Using this equation, the diffusion coefficient of a 692 nm-diameter emulsion droplet is determined to be 7.1 × 10^{-9} cm^2 s^{-1}. The predicted frequency of the benzene

(ZnTPP + IL-PA)/water emulsion droplet collisions is 0.4 Hz. The experimentally observed frequency is 0.14 Hz, and the discrepancy may be caused by the polydispersity of the prepared emulsions and collisions that do not result in a detectable response. The size of the droplets can also be estimated from the electrochemical data and the EDR model. The current transient in a collision event (i.e., current spike) can be integrated versus time to obtain the amount of charge for the oxidation of ZnTPP in a single emulsion droplet assuming complete electrolysis of the contents within the droplet. From the calculated charge, we can estimate the size of the collided benzene (ZnTPP) droplet. We assume that all spherical emulsion droplets contain 5 mM ZnTPP, and the total consumption of all the ZnTPP molecules during a collision. Eq 3 is then used to calculate the droplet diameter (d_{drop}):[15]

$$d_{drop} = \sqrt[3]{\frac{6Q}{\pi n F C_{redox}}} \tag{3}$$

where Q is the integrated charge from the spiked peak, n is the number of electrons transferred per molecule, F is the Faraday constant, and C_{redox} is the redox species concentration in the dispersed phase. The calculated diameter is displayed in Figure 3E (red bars). The size distribution based on the electrochemical measurements agrees with the DLS result (black line in Figure 3E), implying that the assumption of bulk electrolysis was reasonable for the interpretation of the electrochemical results. Under our experimental conditions, the minimum size for droplet collision detection was approximately 500 nm. Moreover, the electrochemical measurements detected some large droplets (1200−5000 nm) that were not detectable via the DLS methodology, demonstrating the advantage of the electrochemical strategy presented here.

i−t Decay Behavior of the ZnTPP in the Benzene (ZnTPP) Emulsion Droplets. In prior research on a ferrocene in toluene emulsion and a TCNQ in nitrobenzene emulsion, the
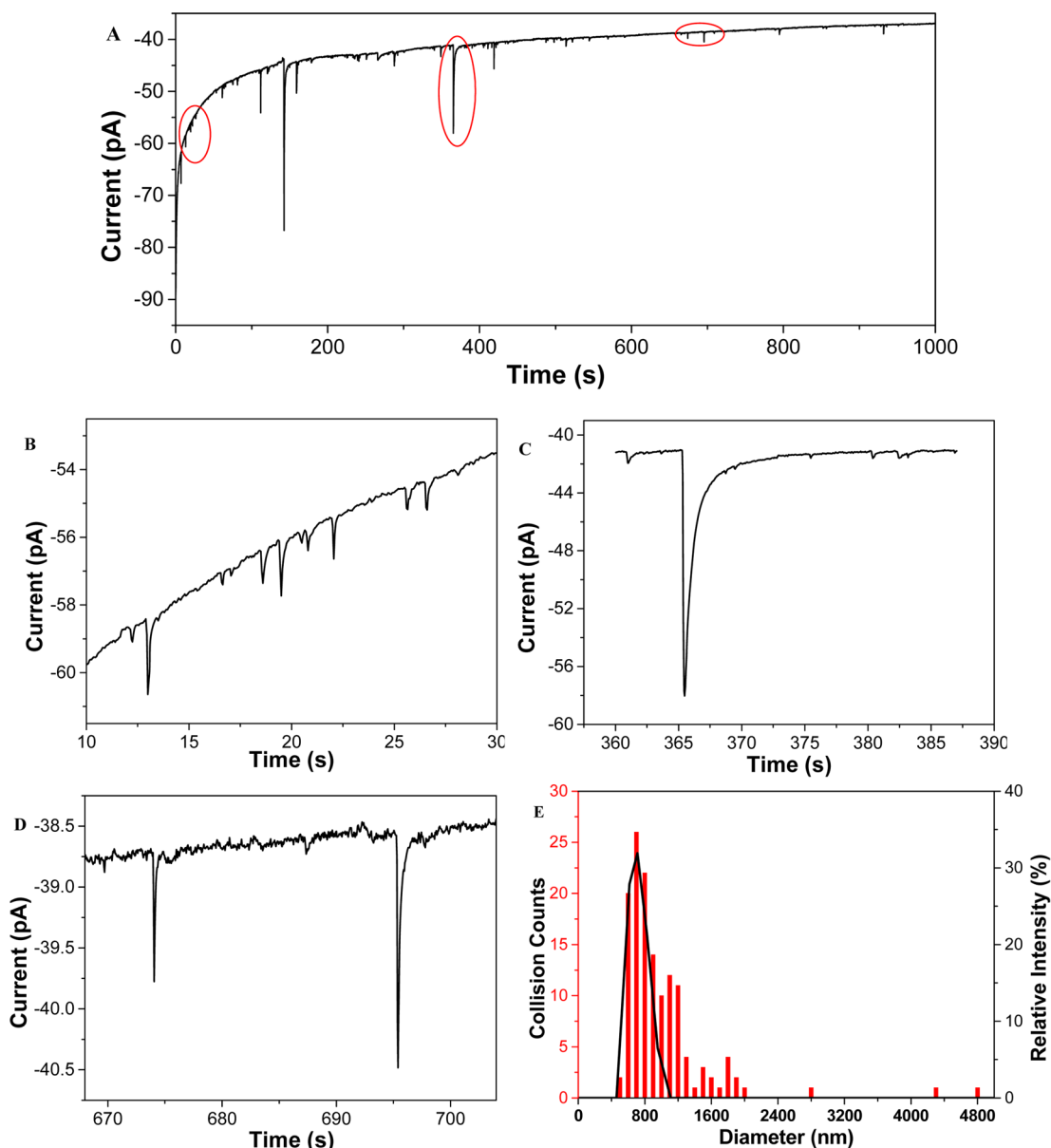
Figure 3. (A) Amperometric $i-t$ curve of the emulsion droplet collisions on the Au UME. The measurement mixture contains ca. 46.7 pM benzene (ZnTPP) emulsion droplets in benzene-saturated water. (B−D) Magnified $i-t$ curves showing the clear spike-type responses. The Au UME was biased at +0.65 V vs. Ag wire during the entire experimental time. (E) Comparison of the droplet size distribution from eq 3 (red bars) vs. the DLS data (black line).

electrolysis of the redox molecule in a single emulsion droplet demonstrated similar behavior to the bulk electrolysis in which the current decayed exponentially with time.[15,16] The model assumes that the droplet attaches itself to the colliding surface upon collision, opening up and exposing its contents to a small disk electrode for electrolysis. Similarly, we could still use the bulk electrolysis model to explain the emulsion system for ZnTPP oxidation (Figure 4). Eqs 4 and 5 describe the $i-t$ behavior of the bulk electrolysis,[30]

$$m = \frac{4D_{ZnTPP}}{\pi r_e} \tag{4}$$

$$i(t) = i_p e^{-\left(\frac{mA}{V}\right)t} \tag{5}$$

where m is the mass-transfer coefficient for a disk electrode, D_{ZnTPP} is the diffusion coefficient of the ZnTPP in the benzene

(ZnTPP) emulsion droplets, and r_e is the effective contact radius between the UME and the emulsion droplet upon collision. m is subsequently used in eq 5. Here, i_p is the peak current, A is the effective contact area between the UME and the emulsion droplet calculated from r_e, V is the volume of the droplet calculated from the diameter of the droplet, d_{drop}, and t is the electrolysis time. By combining eqs 4 and 5, a relation (eq 6) is found between the electrolysis time and the electrolysis current:[30]

$$i(t) = i_p e^{-\left(\frac{4r_e D_{ZnTPP}}{V}\right)t} \tag{6}$$

D_{ZnTPP} is calculated from the cyclic voltammogram in Figure S2 using eq 7,
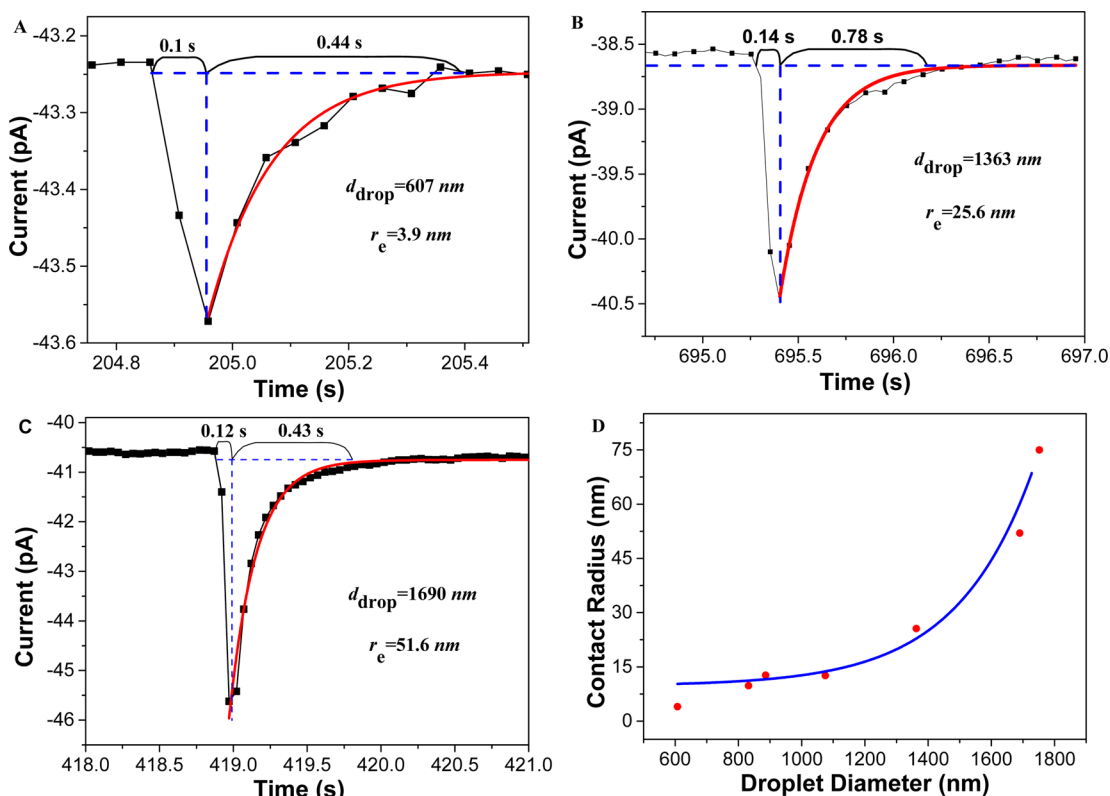
Figure 4. (A−C) Zoomed-in i−t curve and analysis of the single current spike. The experimental data were sampled every 50 ms (black squares). The fitted i−t decay behavior (red lines) was obtained using eq 6 and by performing nonlinear regression analysis with an exponential model. The d_{drop} and r_e are calculated from the integrated charge and eqs 3 and 8, respectively. (D) The plot of the contact radius (r_e) vs. the droplet diameter (d_{drop}) of the benzene (ZnTPP) emulsion droplet. The red solid circles represent the values of contact radius calculated using eq 6 and the best fit curve (eq 8). The blue line is the nonlinear regression plot for the exponential decay model.

$$D_{ZnTPP} = \frac{i_{ss}}{4nFC_{ZnTPP}r_{elec}} \tag{7}$$

where i_{ss} is the steady-state current, C_{ZnTPP} is the concentration of ZnTPP, and the resultant D_{ZnTPP} is 6.60×10^{-7} cm^2 s^{-1}.

When a single droplet lands on an UME, within a very short time (0.1−0.14 s), the droplet is exposed to the UME as a disk with an effective contact radius, r_e (Figure 4A−C). The current follows an exponential decay as a function of time as ZnTPP is consumed via the electrolysis. Assuming that both the droplet volume and the contact radius remain constant during the electrolysis process, we obtained the best-fit i−t decay behavior (red lines) using eq 6 and performed a nonlinear regression analysis with the exponential model. It should be stressed that the chosen redox probes herein are intermediately hydrophobic and they become relatively hydrophilic after oxidation. The concentration of ionic species initially in the aqueous phase is very low considering the hydrophobicity of ionic liquids and absence of supporting electrolyte in the aqueous phase. Moreover, ion transfer across the oil/water interface is a fast/reversible process, which will not complicate the bulk electrolysis model employed in this study. On the basis of all these facts, it is feasible to propose a mechanism of expulsion of oxidized redox probe rather than counteranion ingress from the aqueous phase during electrochemical reaction. It has been seen that theoretical curves all agree well with the experimental i−t curves (black squares in Figure 4A−C), suggesting that the ZnTPP oxidation in the benzene (ZnTPP) emulsion droplet follows the same bulk electrolysis model as the ferrocene oxidation in a toluene emulsion droplet.[15]

The values of $(4r_e D_{ZnTPP})/V$ for droplets of various sizes were obtained from the best fit results (red lines in Figure 4A−C), and accordingly, r_e was calculated on the basis of droplets volume V. r_e is then plotted as a function of d_{drop} in Figure 4D. A nonlinear regression analysis with an exponential model was used to fit the data points and is shown in Figure 4D; the corresponding best fit equation (i.e., calibration curve) is shown as eq 8.

$$r_e = 9.73 + 0.048e^{0.0041d_{drop}} \tag{8}$$

It should be noted that the exponential dependence of r_e on d_{drop} is an experimentally observed relationship and is not derived rigorously on the basis of a physical model. When 64.6 pM of emulsion was introduced into the system, similar results were observed as discussed above (Figure S4). The result shows that the process of oxidizing ZnTPP to ZnTPP$^{\bullet+}$ probably results in the expulsion of ZnTPP$^{\bullet+}$ from the benzene droplet into the water phase to maintain the charge balance. The emulsion method is flexible in that the electroactive material can be changed to be reasonably soluble in benzene. To verify this flexibility, we also employed Fc, DMFc, and CuTPP as the redox species. The corresponding i−t curve and DLS data are provided in Figures S5, S6, and S7. The size distribution from the electrochemical measurements (red bars in Figures S5B, S6B, and S7B) agrees with the DLS result (black lines in Figures S5B, S6B, and S7B). These results suggest that the hydrophobic electroactive material oxidation in the benzene emulsion droplet follows the bulk electrolysis model.

Collision Frequency as a Function of the Concentration of the Benzene (ZnTPP) Emulsion Droplet. Figure 5 displays a
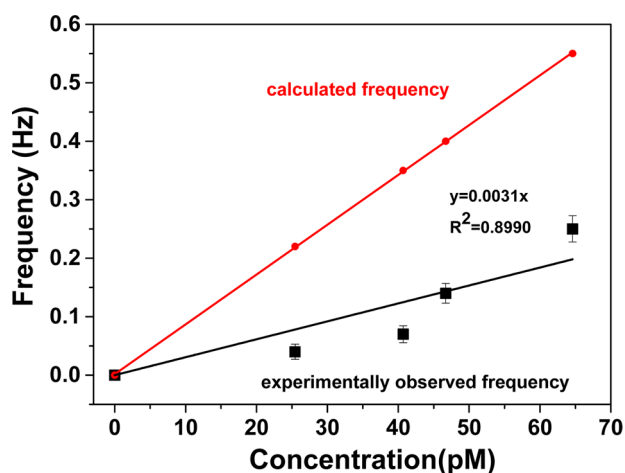

Figure 5. Collision frequency as a function of concentration of the benzene (ZnTPP) emulsion droplet. The error bars correspond to the standard deviation at three measurements. The potential was held at +0.65 V vs. Ag wire.

plot of the collision frequency versus different concentrations of the benzene (ZnTPP) emulsion droplet. In Figure 5, the experimental and theoretical results for the collision frequency as a function of the concentration of the benzene (ZnTPP) emulsion droplet are compared. As expected, we observe a linear relationship between collision frequencies versus the concentration of droplets in the system. The experimentally observed frequency is two times smaller than the calculated frequency. The difference between the calculated and experimentally observed frequency is within the usual variations of measurements of stochastic events. This result suggests that the collision of droplets is mainly governed by diffusion.[16] Research addressing the quantitative determination of biologically relevant materials using the proposed collision technique is actively being pursued.

Single-Collision Events of the Cyclohexane Emulsion Droplets. *Electrochemical Oxidation of Fc in the Bulk Cyclohexane Solution with 400 mM IL-PA as Supporting Electrolyte.* Normally, solvents used in electrochemical studies need sufficient conductivity to minimize the Ohmic drop in bulk solution, and then, the potential applied at the working electrode/electrolyte interface is effective. Cyclohexane has a dielectric constant of 2.02 and is usually not possible for electrochemical studies because of this low dielectric constant. Since such low-dielectric-constant solvent cannot dissolve or dissociate the conventional ionic electrolytes effectively, electrochemistry data in cyclohexane and analogues is scarce. To alleviate this difficulty, we again chose the IL-PA as the supporting electrolyte. A CV of 20 mM ferrocene (Fc) in neat cyclohexane with 400 mM IL-PA as supporting electrolyte was measured with a 10 μm Au UME at a scan rate of 5 mV s^{-1} (Figure S8). The CV shows a sigmoidal wave for the one-electron Fc electrochemical oxidation and is minimally perturbed by the uncompensated resistance ($E_{3/4} - E_{1/4} = 74$ mV). The oxidation of Fc began at approximately +0.4 V (vs. Ag wire) and displays steady-state current at approximately +0.6 V. The same cyclohexane composition in 0.15 mL, mixed with 5 mL of water, was used to prepare the emulsion for the collision experiments. The same acoustic ultrasonication

methodology as that adopted in benzene emulsion preparation was used to form the emulsion, which was stable for at least 16 h.

Collision Experiments of the Cyclohexane Emulsion Droplets on the Gold UME. The collisions of the cyclohexane emulsion droplets were measured using an amperometric $i-t$ curve with 19.8 pM cyclohexane emulsion droplets at a bias potential of +0.6 V on an Au UME (Figure 6). Many large current spikes were observed during the measurement. The electrolysis times for the cyclohexane emulsion droplets (0.43–0.78 s) were similar to those of the benzene (ZnTPP) emulsion droplets (0.42–0.76 s). The diffusion coefficient of a cyclohexane emulsion can be estimated using eq 2 for an 864 nm diameter droplet (5.7 × 10^{-9} cm^2 s^{-1}). The collision frequency was estimated to be f_{ems} = 0.103 Hz. The experimentally observed current spike frequency is slightly smaller than the calculated one (0.14 Hz). The difference between the calculated and experimentally measured values is within the commonly observed variations for measurements of stochastic events, implying that the collisions are primarily governed by the diffusion of the droplets. The d_{drop} was obtained from the integrated charge in combination with eq 3, and the corresponding size distribution is shown in Figure 6E. The electrochemical data fairly agree with the DLS data especially in the smaller size zone. Here, the electrochemical data also revealed some large droplets that were not detected in the DLS measurements, displaying the advantage of the developed methodology presented here.

i–t Decay Behavior of Fc Oxidation in the Cyclohexane Emulsion Droplet during the Collision Measurement. We can also explain the cyclohexane emulsion system for the Fc oxidation electrolysis using the above-mentioned bulk electrolysis model (Figure 7). The diffusion coefficient of Fc in cyclohexane can be calculated from eq 7 and Figure S8, with the resultant D_{Fc} of 2.4 × 10^{-6} cm^2 s^{-1}. The $i-t$ decay of a cyclohexane emulsion droplet upon collision shows similar behavior as bulk electrolysis. Eq 6 for the $i-t$ decay behavior was used to explain the possible dynamic process. When the cyclohexane emulsion droplet collides with an Au UME, the droplet forms a tiny disk electrode with an effective radius r_e. The contact area characterizes the disk electrode because it touches the electrochemical reactor (volume of approximately 337.5 aL). Assuming that both the droplet volume and the contact radius remain constant during the electrolysis process, we obtained the best-fitted $i-t$ decay behavior (red lines) using eq 6 and performed a nonlinear regression analysis with the exponential model. An increase in the contact area will result in an increase in the current amplitude (i.e., peak current) of each current spike for the initial 0.1 s. Once the droplet is stably fixed on the UME, the Fc oxidation currents begin to decay because the Fc in the droplet becomes depleted during the electrolysis. r_e was calculated for droplets of different sizes from the best fit results (red lines in Figure 7A–C), and it is plotted as a function of d_{drop} (diameter of the droplet) in Figure 7D. A nonlinear regression analysis with an exponential model was used to fit the data points and is shown in Figure 7D; the corresponding best fit equation is shown by eq 9.

$$r_e = 3.88 + 0.1976e^{0.0022d_{drop}} \qquad (9)$$

When a 12.9 pM emulsion was introduced into the system, similar results were observed as outlined above (Figure S9). The result shows that the process of oxidizing Fc to Fc$^+$ likely results in the expulsion of Fc$^+$ from the cyclohexane droplet
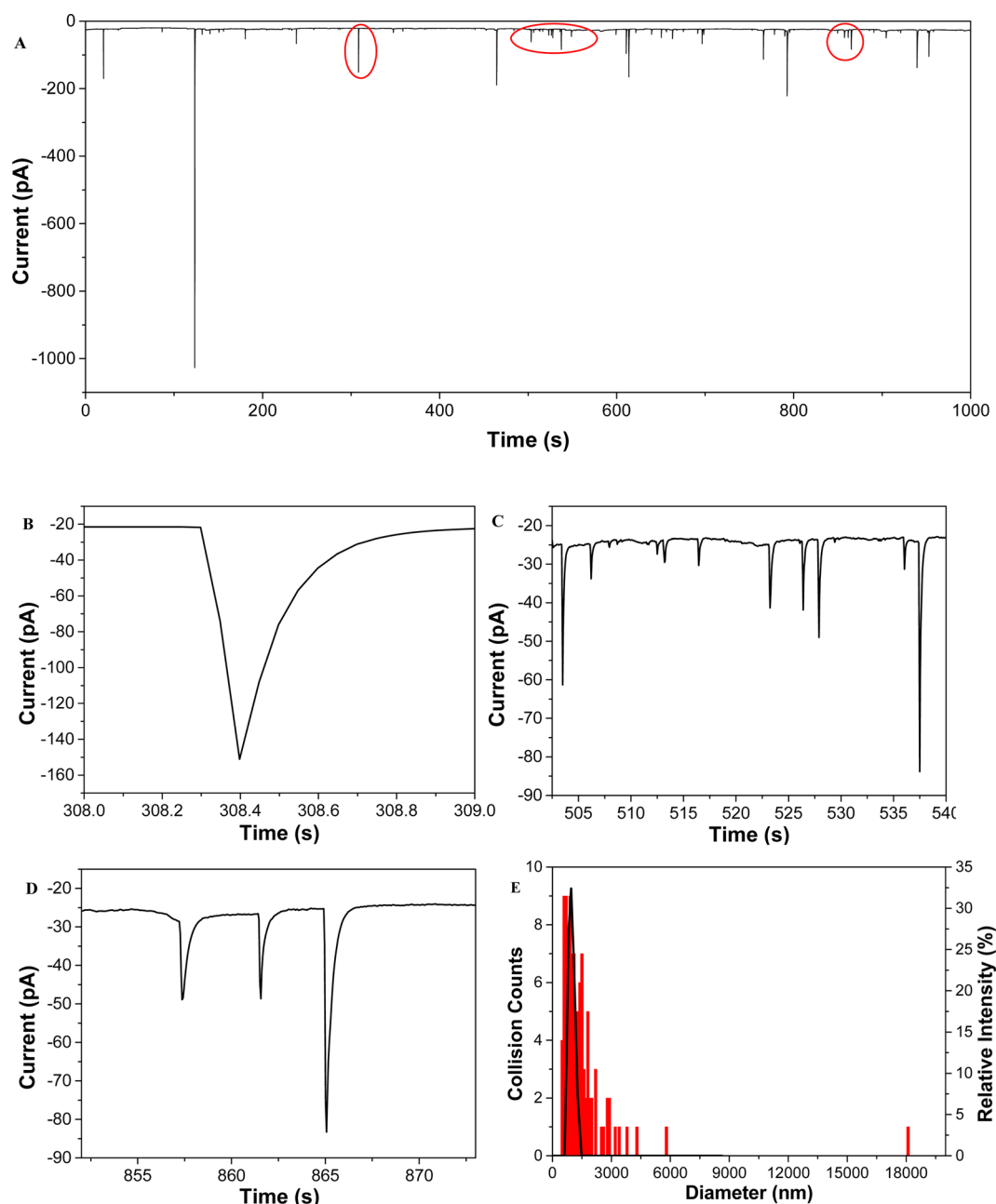
Figure 6. (A) Amperometric *i−t* curve of the emulsion droplet collisions on the Au UME. The test sample contains ca. 19.8 pM cyclohexane (Fc) emulsion droplets and cyclohexane saturated water. (B−D) Magnified *i−t* curves showing clear spiked responses. The Au UME was biased at +0.6 V vs. Ag wire during the entire experimental time. (E) Comparison of the droplet size distribution from eq 3 (red bars) with DLS data (black line).

into the aqueous phase to maintain the charge neutrality in oil phase.

Collision Frequency in Function of the Concentration of the Cyclohexane (Fc) Emulsion Droplet. Figure 8A shows a plot of the collision frequency versus different concentrations of the cyclohexane (Fc) emulsion droplet. In Figure 8A, the experimental and theoretical results for the collision frequency as a function of the concentrations of the cyclohexane (Fc) emulsion droplet are compared. There is a clear contrast between the experimental and theoretical results for collision frequency with the concentration of cyclohexane (Fc) emulsion droplets. Specifically, the experimentally observed frequency is smaller than the calculated frequency using the identical droplet diameter for the whole emulsion concentration range. This

discrepancy could arise from the uncertainty in the value of C_{drop} or migration effects (the zeta potential of the droplet from DLS is −13.5 mV). From Figure 8A (black line), we can also observe that the experimentally observed frequency increases as the concentration of the cyclohexane (Fc) emulsion droplet increases and then the frequency reaches a maximum at a concentration between 20 and 30 pM. The frequency was proportional to the concentration of the emulsion droplets at the lower concentrations (0−~25 pM). However, the frequency decreased when the cyclohexane (Fc) emulsion droplet concentration is further increased (>25 pM), due to the coalescence of small droplets into larger ones (see the DLS data in Figure 8B). Therefore, the method is better fitted to detect low concentrations of cyclohexane (Fc) emulsion droplets.
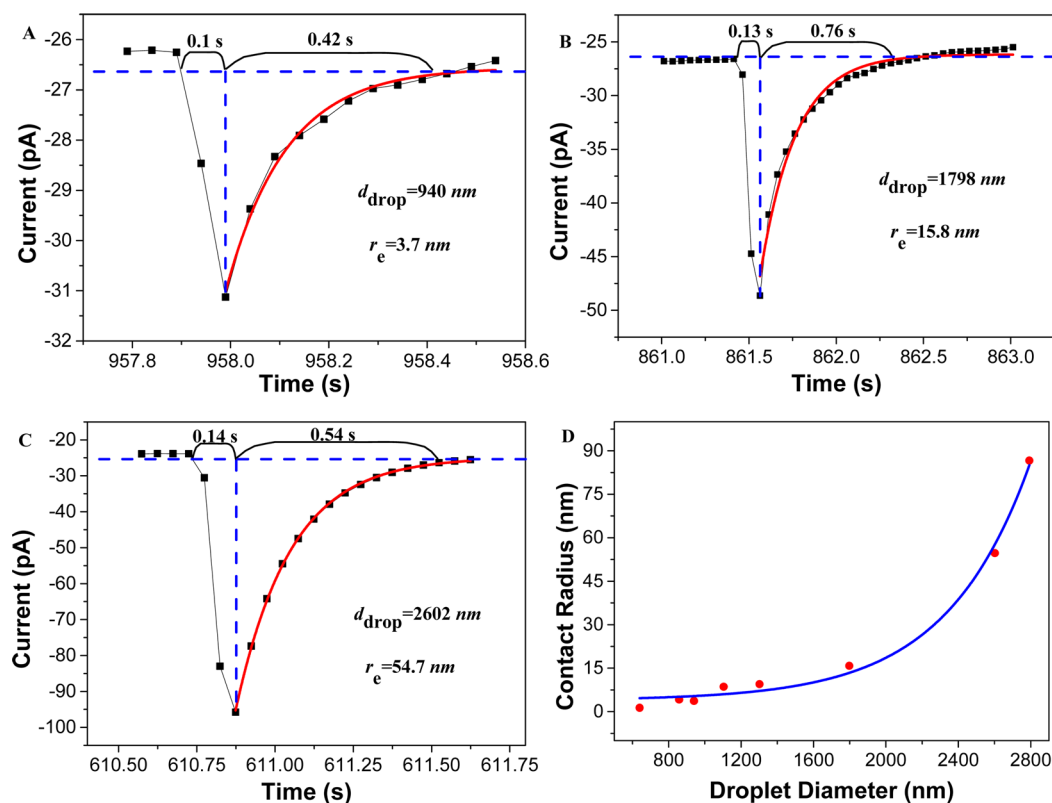
Figure 7. (A–C) Enlarged $i–t$ curve and analysis of single current spike. The experimental data were sampled every 50 ms (black squares). The simulated $i–t$ decay behavior (red lines) was obtained using eq 6 and by computing the nonlinear regression analysis with an exponential model. The d_{drop} is calculated from the integrated charge and eq 3. (D) Plot of contact radius (r_e) vs. droplet diameter (d_{drop}) of the cyclohexane (Fc) emulsion droplet. The red circles represent the values of the contact radius that were calculated using eq 6 and the best fitting line. The blue line is the nonlinear regression plot with the exponential decay model.
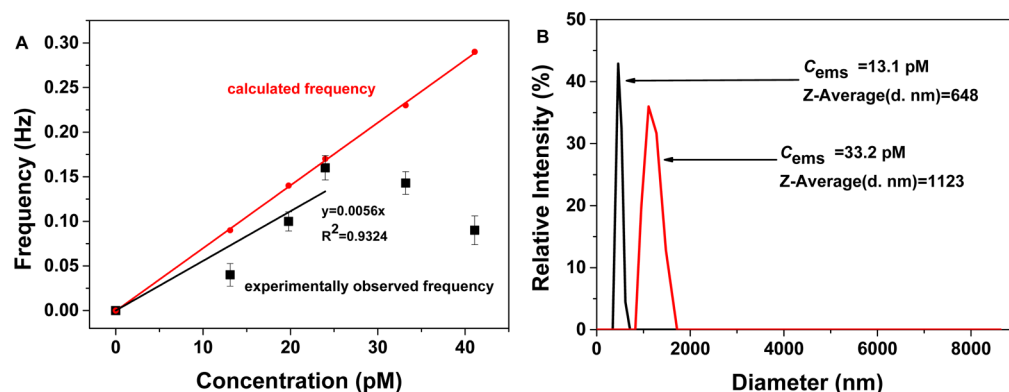

Figure 8. (A) Collision frequency vs. concentration of the cyclohexane (Fc) emulsion droplet. The error bars correspond to the standard deviation at three measurements. The potential was held at +0.6 V vs. the Ag wire. (B) DLS data with different concentrations of the cyclohexane (Fc) emulsion droplet.

■ CONCLUSIONS

We report the electrochemical collisions of single emulsion oil droplets featured with extremely low dielectric constants (e.g., benzene, cyclohexane) as determined via EDR studies on an UME. First, we demonstrated the electrochemical oxidation of a redox molecule, ZnTPP, in benzene emulsion droplets. A spike-type current response was observed when the collisions occurred during the experiment. We quantitatively analyzed the collision response, collision frequency, and size distribution of the emulsion droplets. Subsequently, the $i–t$ decay behavior analysis was also addressed. We also studied the oxidation of

Fc, DMFc, and CuTPP in the benzene emulsion droplets. The results suggest that the hydrophobic electroactive material oxidation in the benzene emulsion droplet follows the bulk electrolysis model. Second, we extended our study to the electrochemical oxidation of a redox molecule, Fc, in cyclohexane emulsion droplets. The results from this collision measurement were quantitatively analyzed in the same manner as for the benzene (ZnTPP) emulsion system. A probable mechanism of the Fc oxidation in the cyclohexane emulsion droplet was discussed. The work presented herein has demonstrated that bulk electrolysis can be achieved in a few seconds in these attoliter reactors, which corroborated the

earlier work of toluene emulsions,[15] and it will stimulate many other applications, such as electrosynthesis in low dielectric constant solvents that exhibit a much broader potential window. These novel concepts and the experimental studies reported here increase the understanding of the single droplet electrochemistry and will promote new practical applications.

■ ASSOCIATED CONTENT

Ⓢ Supporting Information

The Supporting Information is available free of charge on the ACS Publications website at DOI: 10.1021/acs.anal-chem.5b02968.

Additional figures and photographs (PDF)

■ AUTHOR INFORMATION

Corresponding Author

*E-mail: ajbard@mail.utexas.edu. Fax: (512) 471-0088.

Notes

The authors declare no competing financial interest.

■ ACKNOWLEDGMENTS

■ REFERENCES

(1) Kleijn, S. E. F.; Lai, S. C. S.; Koper, M. T. M.; Unwin, P. R. *Angew. Chem., Int. Ed.* **2014**, *53*, 3558−3586.

(2) Xiao, X.; Fan, F.-R. F.; Zhou, J.; Bard, A. J. *J. Am. Chem. Soc.* **2008**, *130*, 16669−16677.

(3) Kim, J.; Kim, B.-K.; Cho, S. K.; Bard, A. J. *J. Am. Chem. Soc.* **2014**, *136*, 8173−8176.

(4) Zhou, Y. G.; Rees, N. V.; Compton, R. G. *Angew. Chem., Int. Ed.* **2011**, *50*, 4219−4221.

(5) Zhou, H.; Fan, F.-R. F.; Bard, A. J. *J. Phys. Chem. Lett.* **2010**, *1*, 2671−2674.

(6) Zhou, Y.-G.; Haddou, B.; Rees, N. V.; Compton, R. G. *Phys. Chem. Chem. Phys.* **2012**, *14*, 14354−14357.

(7) Haddou, B.; Rees, N. V.; Compton, R. G. *Phys. Chem. Chem. Phys.* **2012**, *14*, 13612−13617.

(8) Kwon, S. J.; Fan, F.-R. F.; Bard, A. J. *J. Am. Chem. Soc.* **2010**, *132*, 13165−13167.

(9) Fosdick, S. E.; Anderson, M. J.; Nettleton, E. G.; Crooks, R. M. *J. Am. Chem. Soc.* **2013**, *135*, 5994−5997.

(10) Sardesai, N. P.; Andreescu, D.; Andreescu, S. *J. Am. Chem. Soc.* **2013**, *135*, 16770−16773.

(11) Park, J. H.; Thorgaard, S. N.; Zhang, B.; Bard, A. J. *J. Am. Chem. Soc.* **2013**, *135*, 5258−5261.

(12) Cheng, W.; Zhou, X. F.; Compton, R. G. *Angew. Chem.* **2013**, *125*, 13218−13220.

(13) Quinn, B. M.; van't Ho, P. G.; Lemay, S. G. *J. Am. Chem. Soc.* **2004**, *126*, 8360−8361.

(14) Stuart, E. J.; Tschulik, K.; Batchelor-McAuley, C.; Compton, R. G. *ACS Nano* **2014**, *8*, 7648−7654.

(15) Kim, B.-K.; Boika, A.; Kim, J.; Dick, J. E.; Bard, A. J. *J. Am. Chem. Soc.* **2014**, *136*, 4849−4852.

(16) Kim, B.-K.; Kim, J.; Bard, A. J. *J. Am. Chem. Soc.* **2015**, *137*, 2343−2349.

(17) Cheng, W.; Compton, R. G. *Angew. Chem.* **2014**, *126*, 14148−14150.

(18) Dick, J. E.; Hilterbrand, A. T.; Boika, A.; Upton, J. W.; Bard, A. J. *Proc. Natl. Acad. Sci. U. S. A.* **2015**, *112*, 5303−5308.

(19) Dunevall, J.; Fathali, H.; Najafinobar, N.; Lovric, J.; Wigström, J.; Cans, A.-S.; Ewing, A. G. *J. Am. Chem. Soc.* **2015**, *137*, 4344−4346.

(20) Dick, J. E.; Renault, C.; Bard, A. J. *J. Am. Chem. Soc.* **2015**, *137*, 8376−8379.

(21) Schramm, L. L. *Emulsions, Foams, and Suspensions: Fundamentals and Applications*; Wiley-VCH: Weinheim, 2005.

(22) Mcclements, D. J. *Crit. Rev. Food Sci. Nutr.* **2007**, *47*, 611−649.

(23) Zhu, X.; Fryd, M. M.; Huang, J.-R.; Mason, T. G. *Phys. Chem. Chem. Phys.* **2012**, *14*, 2455−2461.

(24) Johnson, C. S.; Gabriel, D. A. *Laser Light Scattering*; Dover: New York, 1981.

(25) Mason, T. G.; Wilking, J. N.; Meleson, K.; Chang, C. B.; Graves, S. M. *J. Phys.: Condens. Matter* **2006**, *18*, R635−R666.

(26) Dick, J. E.; Renault, C.; Kim, B.-K; Bard, A. J. *Angew. Chem., Int. Ed.* **2014**, *53*, 11859−11862.

(27) Dick, J. E.; Renault, C.; Kim, B.-K; Bard, A. J. *J. Am. Chem. Soc.* **2014**, *136*, 13546−13549.

(28) Howell, J. O.; Wightman, R. M. *J. Phys. Chem.* **1984**, *88*, 3915−3918.

(29) Xiao, X.; Bard, A. J. *J. Am. Chem. Soc.* **2007**, *129*, 9610−9612.

(30) Bard, A. J.; Faulkner, L. R. *Electrochemical Methods, Fundamentals and Applications*, 2nd ed.; John Wiley & Sons: New York, 2001.